International Journal of Medical, Medicine and Health Sciences
ISSN: 2517-9969
Vol:5, No:11, 2011

Real-Time Image Analysis of Capsule Endoscopy for Bleeding Discrimination in Embedded System Platform

Yong-Gyu Lee and Gilwon Yoon*

***Abstract*—**Image processing for capsule endoscopy requires large memory and it takes hours for diagnosis since operation time is normally more than 8 hours. A real-time analysis algorithm of capsule images can be clinically very useful. It can differentiate abnormal tissue from health structure and provide with correlation information among the images. Bleeding is our interest in this regard and we propose a method of detecting frames with potential bleeding in real-time. Our detection algorithm is based on statistical analysis and the shapes of bleeding spots. We tested our algorithm with 30 cases of capsule endoscopy in the digestive track. Results were excellent where a sensitivity of 99% and a specificity of 97% were achieved in detecting the image frames with bleeding spots.

***Keywords*—**bleeding, capsule endoscopy, image processing, real time analysis

I. Introduction

CAPSULE endoscopy provides convenience in endoscopic diagnosis. For instance, a patient can perform daily activities during diagnosis [1]. In particular, it can view all the digestive tract including the small intestine which was difficult to take images by other means [2]. The endoscopic capsule sends the images as it moves along in the digestive track. At the same time, a RF transmitter in the capsule relays measured image data to a receiver that is attached outside of the body. Normally, the capsule operates for 8 hours with three frames (images) per second [3]. About 86,000 image frames are acquired while the capsule passes through the digestive track. It is not easy to analyze this amount of medical images by physicians. When physicians examine with naked eye, they may have misjudgment due to the large amount of data as well as out of fatigue even for one patient [4,5]. The result ends up with an unrecoverable situation to patients and physicians. Therefore, bleeding detection becomes even more important because bleeding is related with many diseases. Unfortunately, it is difficult to differentiate bleeding region from neighboring area and therefore it has a high rate of erroneous diagnosis. For this reason, a support system or tool for image analysis of capsule endoscopy can be very valuable not only for physicians but for patients.There can be two ways of image analysis. One is to process data after all the data are measured and stored. This method has a merit of storing raw data. However, a very large memory is needed and it will take many hours of examination. The other one is real-time processing. The real-time processing deals with much smaller size of data and analysis time can be also reduced substantially. Of course, there are a few challenges for an embedded system of the receiver to detect bleeding. First, illumination in the capsule is not uniform because a limited number of LEDs are used. Others are communication disruption, the degree of blood coagulation and so forth. For these reasons, blood does not show a unique feature. In order to classify various bleeding regions, even under real-time detection, computation and required memory size are burdensome for an embedded system of the receiver.

In this study, we investigated a real-time bleeding detection algorithm based on an embedded system whose memory size and operation capability are limited. An algorithm of categorizing bleeding from its statistical distributions and morphological features was developed. Verification of the algorithm was demonstrated using the images of endoscopic capsules. Section II covers investigations for the patterns and characteristics of bleeding. We introduced a detection algorithm in Section III. Section IV shows the results following by the conclusion section.

II. Bleeding Discrimination

A. Various Features of Bleeding

Bleeding spots do not show in the same color or shape. There are several reasons. Bleeding exhibits various patterns depending on the types of disease. Blood color itself changes depending on oxygenation. Blood color becomes from light red to dark red as the percentage of oxy-hemoglobin decreases [6]. Fig. 1 shows this color change clearly. Another factor is the amount of blood in tissue. Tissue with more blood tends to be lighter red compared to tissue with less blood. This example is shown in Fig. 2. In addition, blood is often mixed with residuals and the color becomes darker red.

In spite of various appearances, bleeding has some common features. In the view of color, red is the center color of blood. In view of chroma, blood tends to be turbid. In terms of brightness, bleeding region is darker than normal tissue [7, 8].

Y-G Lee is with Seoul National University of Science and Technology, Seoul, KOREA (e-mail: yglee@seoultech.ac.kr).

G. Yoon is also with Seoul National University of Science and Technology, Seoul, KOREA (phone: 82-2-970-6419; fax: 82-2-979-7903; email: gyoon@seoultech.ac.kr). *Correspondence to G. Yoon.

B. Change of Tissue distribution depending on brightness

There can be always imbalance of brightness because of the position or posture of the capsule in the duct, the instability of LED intensity and varied sensitivities of image sensors. This influences the process of image analysis and they are;

- Change of RGB distribution on biological tissue
- Changes of optical properties of tissue
- Decrease of brightness on bleeding area
- Inability of image processing due to over- or under-illumination

The influences of the above factors are significant. There are some cases of being unable to examine the images due to over- or under-illumination on a particular spot or the whole image [9]. Such unreadable spots reduce the accuracy of blood detection algorithm since there is no available information. The distribution changes in the optical properties make the optical characteristics of normal tissues similar to those of bleeding under different conditions of illumination. In this case, detection reliability deteriorates if bleeding detection is based on the optical characteristics. Naturally, an algorithm of finding bleeding spots should be very sophisticated and cannot be handled by a microcontroller in the embedded system any more. Fig. 3 illustrates a typical example of distribution changes caused by non-uniform illumination. RGB distributions at different spots vary even though they are the same tissue. For some other cases, it is difficult to examine even with naked eye if illumination is not enough. However, the intensity ratios among the frequencies remain about the same even if illumination varies. We will utilize this point to develop detection algorithms.

C. Constraints of Embedded System

For real time processing, we have to use an embedded system in the receiver which has limitations in memory and operational capability. Methods based on training data or statistical analysis using principal component analysis and partial least squares regression are not adequate. Therefore, it is preferred to have less computation with smaller memory size.

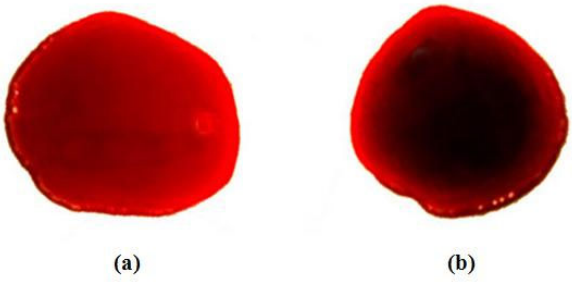

Fig. 1 Color of red blood cell; (a) high oxy-hemoglobin concentration, (b) low oxy-hemoglobin concentration. Red blood cell becomes darker as oxygenation decreases

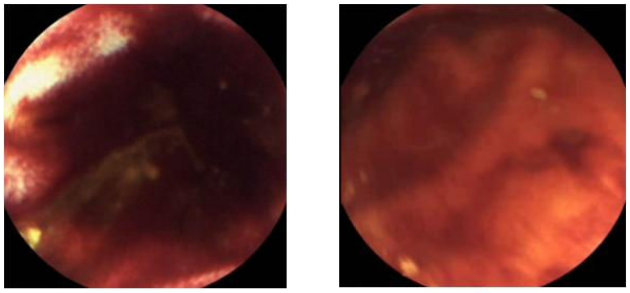

Fig. 2 Difference in brightness depending on the amount of blood; (a) has more blood in tissue than (b)

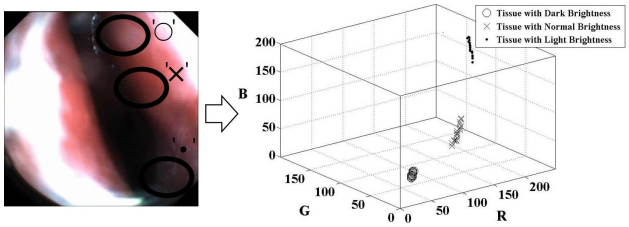

Fig. 3 Changes of the RGB distribution of the same tissue due to unbalanced illumination. It shows that distributions are not in the same location

III. Methodology

Fig. 4 shows the overall process of bleeding detection in real time. In order to use smaller memory size and less computation, the frame was divided into blocks and statistical features of bleeding were extracted. First we analyzed many bleeding regions and found certain features to be discussed in the later section and set threshold values. Morphological filtering was used to extract morphological characteristics on the clustered shape of bleeding inside a particular image.

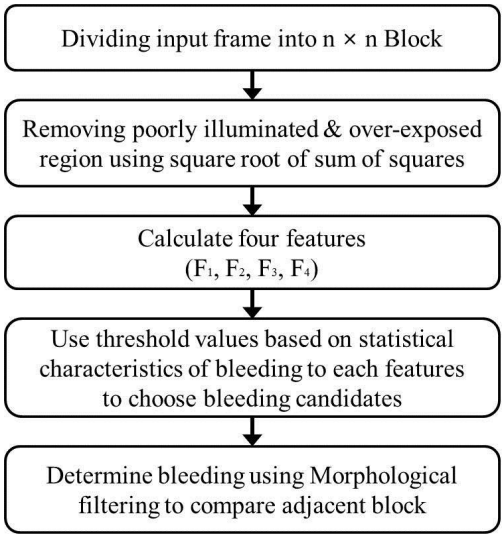

Fig. 4 Overall process for bleeding discrimination

A. Removal of Dark & Bright Blocks

There can be certain blocks in the digestive track image that cannot be processed. For examples, they are dark and bright spots including those of under- or over-illumination. Air bubbles belong to this category. It is necessary to remove these regions. Eq. (1) represents luminance that is defined as the root of sum of the RGB squares. This calculation was done for every block. Blocks under or above certain thresholds were masked.

$$I_{Block}(i,j) = \sqrt{R^2_{Block}(i,j) + G^2_{Block}(i,j) + B^2_{Block}(i,j)} \quad (1)$$

where i, j is horizonal and vertical index in the frame

B. Selection of Features

We introduced several features which can differentiate bleeding from normal tissue. Optical frequency bands are 630-780 nm for R, 490-560 nm for G and 450-490 nm for B. Blood has high reflectivity for R whereas G and B have lower reflectivity. G and B have similar reflectivity and the image sensor detector shows little difference between them. We selected the ratio of R with respect to the vector amplitude of G and B for each block. This feature was designated as F_1. F_1 is expressed by Eq. (2). F_2 was the vector amplitude of G and B and shown in Eq. (3). Difference between G and B was defined as F_3 and is shown in Eq. (4). Bleeding has a higher proportion in terms of chroma compared to normal tissue and, therefore, this was assigned as another feature. This is F_4 and is given in Eq. (5).

$$F_1(i,j) = \frac{R_{Block}(i,j)}{\sqrt{G^2_{Block}(i,j) + B^2_{Block}(i,j)}} \quad (2)$$

$$F_2(i,j) = \sqrt{G^2_{Block}(i,j) + B^2_{Block}(i,j)} \quad (3)$$

$$F_3(i,j) = \left| G_{Block}(i,j) - B_{Block}(i,j) \right| \quad (4)$$

$$F_4(i,j) = 1 - \frac{\min(G_{Block}(i,j), B_{Block}(i,j))}{R_{Block}(i,j)} \quad (5)$$

C. Threshold based on Statistical Distribution of Features

Bleeding does not show a unique pattern and exhibits various distributions in the color map due to the cause of bleeding, lighting, residuals in the digestive duct and so forth. The influence of dark or bright color is significant during analyzing the images. Therefore, detection of bleeding may result in high misjudgment rates if only a certain value of threshold is set. We believe that the algorithms should consider the influence of illumination in detecting bleeding.

Mostly, bleeding has a dominant value of R and the illumination of bleeding is closely related with R values [10]. A threshold was assigned depending on the amplitude of dominant R. We studied statistical distributions of all the features ($F_1 \sim F_4$) for bleeding samples and set the values of threshold. For this purpose, 20 bleeding samples each of which had 120 x 120 pixels were used.

Fig. 5 shows the mean and standard deviation for F_1. As shown in the figure, there were no values of R that was under 23 or above 223. It means that no bleeding distributions exist due to under- and over-illumination respectively. For higher R values, the mean of F_1 increases at a slower rate and the standard deviation becomes smaller as R increases. Thus, considering the mean and standard deviation, the threshold for F_1 (i.e., T_1) was set as in Eq. (6). In this study, a_1 was 0.003 and b_1 was 1.36. F_1 higher than the threshold was classified as bleeding.

$$T_1(R(i,j)) = a_1 R(i,j) + b_1 \quad (6)$$

Fig. 6 illustrates a profile of values of means and standard deviations for F_2. Mean of F_2 also increases as R increases. Above higher than 150, the increase of the mean slows down. On the other hand, the standard deviation rather increases. In other words, F_2 distribution becomes wider.

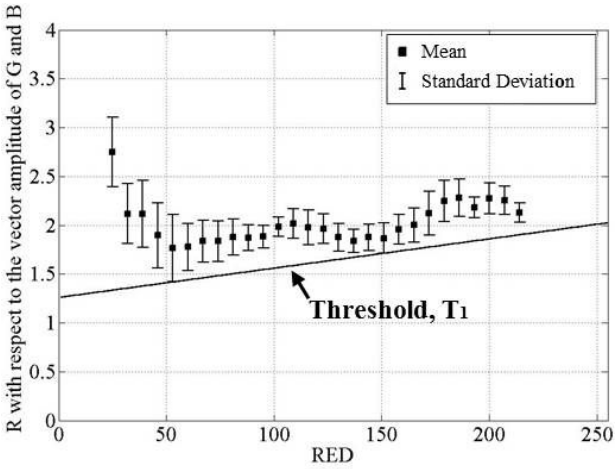

Fig. 5 Mean and standard deviation of bleeding samples for Feature F_1, R with respect to the vector amplitude of G and B

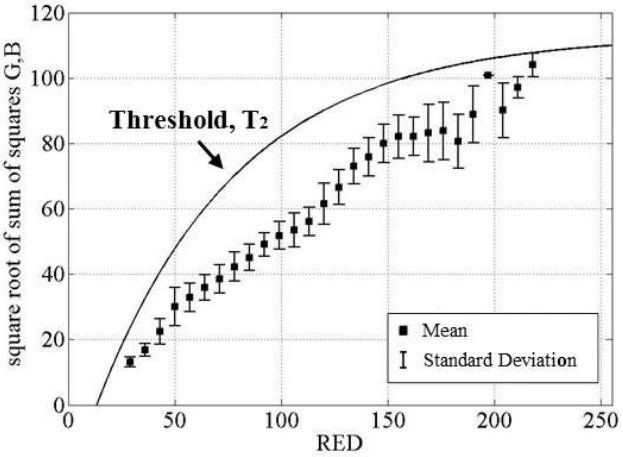

Fig. 6 Mean and standard deviation of bleeding samples for Feature F_2, the root of sum of squares for G and B

An exponential function was adapted to set a threshold equation for F_2 , i.e., T_2 as given in Eq. (7). In our study, we set $a_2 = 138$, $b_2 = -25$ and $c_2 = -0.015$.

$$T_2(R(i,j)) = a_2(1 - e^{c_2 R(i,j)}) - b_2 \quad (7)$$

Fig. 7 shows F_3 in terms of the mean and standard deviation. As R increase, the mean of F_3 increases. The standard deviation also becomes bigger with much higher rates. Thresholds for F_3 (T_3) were expressed as given in Eq. (8). T_3 is shown in solid line in Fig. 7 when we assigned a_3 as 52, b_3, -7.5 and c_3, -0.015. Values less than T_3 were diagnosed as potential bleeding spots.

$$T_3(R(i,j)) = a_3(1 - e^{c_3 R(i,j)}) - b_3 \quad (8)$$

Fig. 8 shows Feature F_4 for bleeding with respect to the mean and standard deviation. F_4 was rather independent on R values. Getting the most out of Fig. 8, we set a first order equation as T_4 (F_4 threshold) instead of having a constant value. Fig. 8 shows the threshold line when $a_4 = 0.0009$ and $b_4 = 0.51$.

$$T_4(R(i,j)) = a_4 R(i,j) - b_4 \quad (9)$$

In order to be diagnosed as the final bleeding candidates, the bleeding conditions of all four features should be met.

D. Classification in the spatial views

There is an addition criterion to be diagnosed as bleeding spot finally. There can be erroneous diagnosis for potential bleeding spots when they are determined only from the features. There are very small spots like noises and they tend to exist alone. They are also randomly distributed [11,12]. On the other hand, bleeding regions tend to be clustered in the scale of pixel size. Therefore, the candidates for bleeding spot were checked whether they were in any clustered formation.

To check whether a final bleeding candidate was in a clustered formation or not, a binary matrix was formulated with the neighboring blocks. Morphological filtering was performed using a 5 by 5 mask. This mask was formulated by the binary matrix made through the neighboring blocks of the bleeding candidate. The mask is shown in Eq. (10).

In our case, we diagnosed a block as bleeding spot when the output of the binary matrix is higher than 0.5. It meant that a block of potential bleeding was diagnosed as such only when the neighboring blocks of potential bleeding existed. We found that erroneous spots were eliminated by doing this process. In addition, we could correct some bleeding blocks in a bleeding region that were incorrectly diagnosed as non-bleeding blocks.

$$M = \frac{1}{25}\begin{vmatrix} 1 & 1 & 1 & 1 & 1 \\ 1 & 1 & 1 & 1 & 1 \\ 1 & 1 & 1 & 1 & 1 \\ 1 & 1 & 1 & 1 & 1 \\ 1 & 1 & 1 & 1 & 1 \end{vmatrix} \quad (10)$$

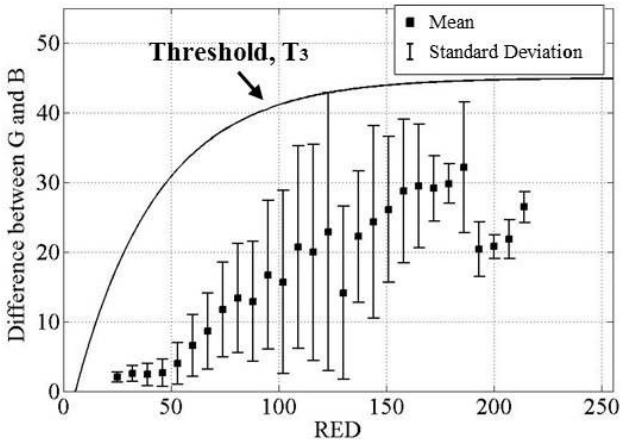

Fig. 7 Mean and standard deviation of bleeding samples for Feature F_3, the difference between G and B

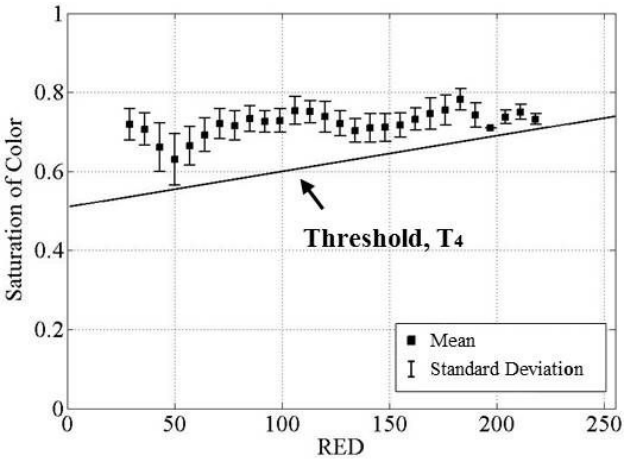

Fig. 8 Mean and standard deviation of bleeding samples for Feature F_4, saturation of color

IV. Results

In order to verify our algorithm, we used 30 cases of endoscopic imaging. 10 out of 30 cases contained bleeding and the rest had no bleeding spots. Each case had 100 frames and the image resolution was 400 x 400 pixels. First, we made blocks where each block had a size of 10 x 10 pixels. Therefore, each frame had 40 × 40 blocks. 30 cases of endoscopy covered a wide range of locality in bleeding spot. Table 1 summarizes the locations of 30 cases.

In this study, we verified the accuracy of our algorithm in detecting frames with bleeding spots in them during video play of endoscopy recordings in real-time. The results were given in terms of sensitivity and specificity as summarized in Table 1.

Sensitivity indicates the capability of finding out the frames with bleeding. Specificity tells us how well we can find out the frames without bleeding spots. Our performance was a sensitivity of 99% and a specificity of 97%.

We have an excellent performance in terms of sensitivity. Often times bleeding regions were dark red and dark red was difficult to diagnose in terms of bleeding detection. However, other bleeding spot in the same frame were well diagnosed as bleeding. Therefore, an overall performance of detecting the frames with bleeding was exceptionally high.

Specificity was also high although stomach imaging has a lower specificity compared to other regions. It turns out that gastric rugae produced non-uniform lighting. It is expected that this was responsible for reduced performance.

V. Conclusion

In this study, we developed a bleeding detection algorithm. The program automatically determined the image frames with bleeding spots in them. This process should be done at the receiver of capsule endoscopy. This means that there are definite limitations of memory size and computational power. In order to come over these challenges, we extracted statistical characteristics of bleeding regions and we called them features. Along with the features, we also utilized morphological characteristics of bleeding regions such as clustered formation. We tested our method with 30 cases of endoscope imaging. The performance of detecting the image frames of bleeding was excellent where the sensitivity was 99 % and the specificity was 97 %.

Acknowledgment

This work has been supported by Bilateral international cooperative research and development program, Ministry of Knowledge Economy, Republic of Korea. We appreciate very much Mr. Y. D. Seo at Intromedic Co., Seoul, Korea for providing with the endoscope images.

References

[1] D. G. Adler and C. J. Gostout, "Wireless Capsule Endoscopy", *Hospital Physician*, 2003, pp.14-22.

[2] A. karargyris and N. Bourbakis, "ASurvey on WCE Imaging Systems and Techniques," *IEEE Engineering in Medicine and Biology Magazine*, Vol. 29, no. 1, 2010

[3] Intromedic Co., South Korea, www.intromedic.com.

[4] N. Bourbakis, "Detecting abnormal patterns in WCE images," in *5th IEEE Symp. on Bioinformatics and Bioengineering (BIBE'05)*, Minneapolis, 2005, pp. 26–29.

[5] B. Li and M. Q.-H. Meing, "Analysis of the gastrointestinal status from wireless capsule endoscopy images using local color feature," in *Proc. the 2007 Inter. Conf. Information Acquisition*, Korea, 2007, pp. 553–557.

[6] J. G. Webster, *Design of Pulse Oximeters*. Bristol and Philadelphia, CA: Institute of Physics Publishing, 1997, ch. 4.

[7] J. Lee, J. OH,X. Yuan and S.-J. Tang, "Automatic classification of digestive organs in wireless capsule Endoscopy Videos," *in Proceedings of the 2007 ACM symposium on Applied computing*, 2007, pp. 1041-1045.

[8] P. Y. Lau, and P. L. Correia, "Detection of Bleeding patterns in WCE video using multiple features," in *29th Annual Int. Conf. of the IEEE Engineering in Medicine and Biology Society, 2007, pp. 5601-5604.*

[9] B. Giritharan, X. Yuan, J. Liu, B. Buckles, J. Oh and S. J. Tang, "Bleeding Detection from Capsule Endoscopy Videos," in *30th Annu. IEEE EBMS Conf.*, Vancouver, 2008, pp. 4780-4783.

[10] A. Karargyris and N. Bourbakis, "A Methodology for Detection Blood-based Abnormalities in Wireless Capsule Endoscopy Videos," in *8th IEEE Inter. Conf. Bioinformatics and Bioengineering,* Athens, 2008, pp. 1–6.

[11] Y. S. Jung, Y. H. Kim, D. H. Lee and J. H. Kim, "Active Blood Detection in a High Resolution Capsule Endoscopy using Color Spectrum Transformation," in *Int. Conf. BioMedical Engineering and Informatics (BMEI)*, Sanya, 2008, pp. 859-862.

[12] C. K. Poh, T. M. Htwe, L. Li, W. Shen, j. Liu, J. H. Lim, K. L. Chan, and P. C. Tan, "Multi-Level Local Feature Classification for Bleeding Detection in Wireless Capsule Endoscopy images," in 2010 *IEEE conf. on Cybernetics and Intelligent Systems, Singapore , 2010, pp. 76-81.*

Yong-Gyu Lee was born in Seong-nam, South Korea (1984) and received his B.S. degree in electronics and information engineering from Seoul National University of Science and Technology, Seoul, South Korea (2010). He is currently a M.S. student at Seoul National University of Science and Technology and engages in biomedical engineering.

Gilwon Yoon received his B.S. in Electrical Engineering from Seoul National University, Seoul, Korea in 1977 and M.S. and Ph.D. in Electrical and Computer Engineering from the University of Texas at Austin, U.S.A. in 1982 and 1988 respectively. He worked at Samsung Advanced Institute of Technology, Korea between 1992 and 2003. He is with Seoul National University of Science and Technology since 2003.